ChemComm

Accepted Manuscript

This article can be cited before page numbers have been issued, to do this please use: S. Ilic, A. Alherz, C. Musgrave and K. Glusac, *Chem. Commun.*, 2019, DOI: 10.1039/C9CC00928K.

ROYAL SOCIETY OF CHEMISTRY

rsc.li/chemcomm

ROYAL SOCIETY OF CHEMISTRY View Article Online
DOI: 10.1039/C9CC00928K

Journal Name

COMMUNICATION

Importance of Proton-Coupled Electron Transfer in Cathodic Regeneration of Organic Hydrides

Stefan Ilic,[ab‡] Abdulaziz Alherz,[c‡] Charles B. Musgrave[cde] and Ksenija D. Glusac*[ab]

2Received 00th January 20xx,
Accepted 00th January 20xx

DOI: 10.1039/x0xx00000x

www.rsc.org/

Electrochemical regeneration of organic hydrides is often hindered by the rapid dimerization of organic radicals produced as the first intermediates of these electrochemical transformations. In this work, we utilize proton-coupled electron transfer to outcompete the undersired dimerization and achieve successful hydride regenerations of two groups of organic hydrides – acridines and benzimidazoles. This work provides an analysis of the critical factors that control the regeneration pathways of organic hydrides.

Proton-coupled electron transfer (PCET) is a process where protons and electrons are transferred either simultaneously or concertedly. While prominent in many biological systems, PCET is also particularly important in fuel cells and artificial photosynthetic systems, because it enables multi-proton and multi-electron transfer processes required for the desired chemical transformation.[1] Electrochemical fuel-forming processes, such as the hydrogen evolution reaction (HER) and CO_2 reduction to methanol, involve several proton and electron transfers. Hydrides are often used in such processes to catalyze the transfer of electrons in pairs, thus avoiding high energy open-shell intermediates obtained by single electron transfers.[2] As such, electrochemical regeneration of catalytic hydrides with optimal efficiency is essential to obtain a high-performing CO_2 reduction and HER.[3] Metal-based hydrides regenerate their hydridic form through stepwise transfers of electrons and protons, and the mechanism is controlled by metal-ligand complexes and experimental conditions (such as applied potentials, proton source, solvent, etc.).[3c, 4] PCET in the regeneration of metal-free hydrides has not been electrochemically explored signficantly beyond flavins and quinones,[5] despite the significance of NADH and similar hydride donors in natural and artificial hydride transfer processes.[6] While the enzymatic regeneration of NADH occurs through a hydride transfer,[6e] the electrochemical formation of NADH analogues is hindered by the difficulty of protonating the one-electron reduced NAD· radical and its rapid dimerization.[7]

Our groups examined the thermodynamic and kinetic hydride donor abilities of various organic NADH analogues[8] and following a series of systematic studies, recently achieved a selective CO_2 reduction to formate under mild conditions using a recyclable organic benzimidazole hydride.[9] Here electrochemical regeneration pathways are explored for two groups of organic hydrides (RH) – acridines and benzimidazoles (Table 1) – from their respective cations (R^+) as an essential step towards their potential utilization as catalysts. We achieved quantitative hydride regeneration by improving the stability of acridine-based radicals and by facilitating the protonation of benzimidazole-based radicals. This work also provides guiding principles for improving the photochemical regeneration of organic hydrides mediated by inorganic semiconductors that act as hole acceptors.[10]

In order to investigate the regeneration pathways for metal-free NADH-analogues and their applicability in electrochemical reductions of protons and CO_2, we calculated relevant hydricity values (ΔG_{H-}), reduction potentials (E^0) and acidity constants in DMSO as solvent (Table 1). Computational details along with experimental procedures and conditions can be found in the Electronic Supplementary Information (ESI). Our calculated ΔG_{H-} values indicate that benzimidazole hydrides act as strong hydride donors with hydricities that compete with noble-metal hydrides,[11] whereas acridine hydrides have moderate reducing strengths, comparable to that of the NADH-cofactor.[8b] However, the considerable hydride donor ability of benzoimidazoles is accompanied by a high energy cost for its regeneration due to the scaling relationship between $E^0(R^+/R^\cdot)$ and ΔG_{H-}.[8b, 8d] Furthermore, their second reductions $E^0(R^\cdot/R^-)$ often occur at potentials ~0.5 V more negative than their first reduction potenitals (Table 1). Here, we suggest utilizing PCETs to circumvent the scaling relationship by avoiding these high-energy interemediates. Another distinguishing characteristic

[a] Department of Chemistry, University of Illinois at Chicago, Chicago, Illinois 60607, United States.
[b] Chemical Sciences and Engineering Division, Argonne National Laboratory, Lemont, Illinois 60439, United States.
[c] Department of Chemical and Biological Engineering, University of Colorado, Boulder, Colorado 80309, United States.
[d] Department of Chemistry, University of Colorado, Boulder, Colorado 80309, United States.
[e] Materials and Chemical Science and Technology Center, National Renewable Energy Laboratory, Golden, Colorado 80401, United States.
‡ S.I. and A.A. contributed equally to this work.
†Electronic Supplementary Information (ESI) available. See DOI: 10.1039/x0xx00000x

View Article Online DOI: 10.1039/C9CC00928K

Table 1. Model R-H compounds and their calculated acidities, reduction and hydride donor ability constants in DMSO as solvent.

Hydride	pK_a		E^0 (V cs Fc/Fc$^+$)			ΔG_{H^-}	Hydride	pK_a		E^0 (V cs Fc/Fc$^+$)			ΔG_{H^-}
	RH$^{+\cdot}$	RH	R$^+$/R$^\cdot$	R$^\cdot$/R$^-$	RH$^{+\cdot}$/RH			RH$^{+\cdot}$	RH	R$^+$/R$^\cdot$	R$^\cdot$/R$^-$	RH$^{+\cdot}$/RH	
A_1H	-0.4	35.8	-1.04	-1.83	0.25	73.0	B_1H	15.2	63.9	-2.56	-3.38	-0.52	47.0
A_2H	-1.8	34.2	-1.07	-1.79	0.28	72.8	B_2H	12.4	48.2	-2.30	-2.53	-0.44	48.6
A_3H	-1.0	35.0	-1.11	-1.86	0.20	70.3	B_3H	14.9	51.7	-2.60	-2.61	-0.47	44.7
A_4H	-3.4	34.0	-1.33	-1.95	0.18	61.1	B_4H	13.6	53.8	-2.70	-2.81	-0.45	41.7
							B_5H	15.4	50.0	-2.66	-2.55	-0.54	45.2
A_5H	-6.4	35.7	-1.80	-2.15	0.28	46.9	B_6H	18.4	54.4	-2.79	-2.63	-0.54	44.7
							B_7H	21.4	50.6	-2.83	-2.58	-0.96	42.7
A_6H	1.7	41.0	-1.44	-2.21	0.01	61.5	B_8H	16.3	54.1	-2.70	-2.81	0.01	41.9

between these two groups of hydrides is the remarkable difference in the acidity constants (pK_a) of their radical cationic intermediates (RH$^{+\cdot}$) that determine their regeneration pathways. We propose two distinct pathways for the electrochemical generation of organic hydrides: (a) sequential transfer of two electrons followed by a proton transfer (EEP) and (b) sequential electron-proton-electron (EPE) transfer. Our calculated pK_a values predict that all model compounds are reduced via the EEP pathway, while only the benzimidazoles can be reduced via EPE with a reasonable proton source. The computed acidity constants reported in Table 1 indicate the drastic difference in acidity values of the intermediates of both classes. Indeed, this computational analysis corroborates our experimental findings discussed below.

The electrochemical behaviour of a representative acridine (A_2^+) in the absence of proton donors exhibits a reversible reduction peak at –0.97 V (vs. Fc/Fc$^+$), which we assign to R$^+$/R$^\cdot$ conversion based on its calculated $E^0_{R+/R^\cdot}$ potentials (Fig 1, Inset 1). Similar reversible first-reduction properties have been observed for the acridine derivatives A_3^+, A_4^+ and A_5^+ (Fig S2, ESI), which are less susceptible to dimerization due to functionalization at the 4-position, justifying the reversibility of the observed reduction.[7c] In contrast, unsubstituted A_1^+ and A_6^+ exhibit irreversilble R$^+$/R$^\cdot$ conversion due to radical dimerization (Fig S2, ESI), a behavior analogous to the natural NAD$^+$-cofactor.[7e, 7f] Potentials associated with the second electron reduction (R$^\cdot$/R$^-$) are shifted to significantly more negative values and exhibit quasi-reversible and irreversible characteristics. Such irreversible behavior is associated with the protonation of the forming anion by the solvent, as confirmed by the appearance of the A_2H oxidation peak at +0.3-0.6 V (vs. Fc/Fc$^+$) in the anodic scan (Fig 1a; for comparison, the CV of A_2H is shown in Fig S4, ESI). Experiments with two acids of significantly different acidities were performed to investigate the electrochemical regeneration of acridine-based hydrides. In the presence of weak acids (i.e. acetic acid, $pK_{a,\ calc}$ = 12.7, DMSO), a modest shift in the second reduction potential of +0.2 V was observed (Fig 1a). This shift and the partial loss of reversibility displayed in the first reduction peak were assigned to facilitated protonation of the anion to form a hydride, indicating regeneration via EEP. This likely occurs via a stepwise mechanism, due to a lack of a kinetic isotope effect when deuterated acetic acid was used. (Fig S5, ESI) However, the shift was not further improved with higher acid concentrations nor slightly stronger acids. In contrast, the addition of a very strong triflic acid ($pK_{a,calc}$ = −8.6, DMSO) resulted in a concomitant increase in the current density at the first reduction potential and the disappearance of the second reduction peak (Fig 1b), suggesting that strong acids facilitate the EPE mechanism.[12] The formation of the hydride via EPE was confirmed by switching the cathodic potential at −1.2 V and monitoring the presence of the hydride oxidation peak (Fig 1, Inset 2). The radical protonation was further confirmed using UV-Vis absorption spectra of chemically produced $A_2^\cdot$ and its reaction with HBF_4 acid. (See section 2G, ESI)

Bulk electrolysis experiments of B_3^+ with acetic acid (which favors the the EEP mechanism) and HBF_4 (which favors the EPE mechanism) both resulted in successful hydride regeneration of B_3H (Fig S9 and S10). B_3H regeneration using HBF_4 occurred at an applied potential of −1.2 V (vs. Fc/Fc$^+$), while hydride formation using acetic acidrequired a more negative applied potential (-2.0 V vs. Fc/Fc$^+$). Nevertheless, both routes yielded a quantitative hydride recovery due to the successful protonation of the radical (EPE route) and its high stability under anaerobic conditions (EEP route; section 2G, ESI).

Cyclic voltammograms of benzimidazole-based derivatives B_3^+ and B_2^+ (Figs 1c and 1d) display irreversible peaks at the potentials predicted for the first electron reduction R$^+$/R$^\cdot$, as indicated in Table 1. The irreversibility of the first reduction peaks is caused by the tendency of unstable benzimidazole radicals to dimerize, as confirmed by the appearance of oxidation peaks in the reverse scan at potentials that match the calculated potentials of dimers (−0.84 V vs. Fc/Fc$^+$ for B_3^+, ESI section 2A). The addition of acetic acid to B_3^+ prevents undesired dimerization, as indicated by the disappearance of the dimer oxidation peak at −0.84 V vs. Fc/Fc$^+$. Instead, formation of the hydride B_3H is now indicated by the new peak at −0.34 V vs. Fc/Fc$^+$ (Inset 3). Hydride formation was further confirmed with controlled-potential electrolysis, where B_3H was observed by NMR as the sole product (Fig S11, ESI). The protonation of $B_2^\cdot$, (and further hydride regeneration) was achieved only in the presence of a large excess of the acid which is consistent with the lower calculated acidity for for $B_2H^{+\cdot}$.

The mechanism of hydride regeneration in benzimidazoles was investigated using compounds B_4H and B_8H with bulky substituents to impede radical dimerization. In the absence of a proton source, the cyclic voltammogram of B_8^+ exhibits electrochemical properties similar to those of the stable acridi-

View Article Online
DOI: 10.1039/C9CC00928K

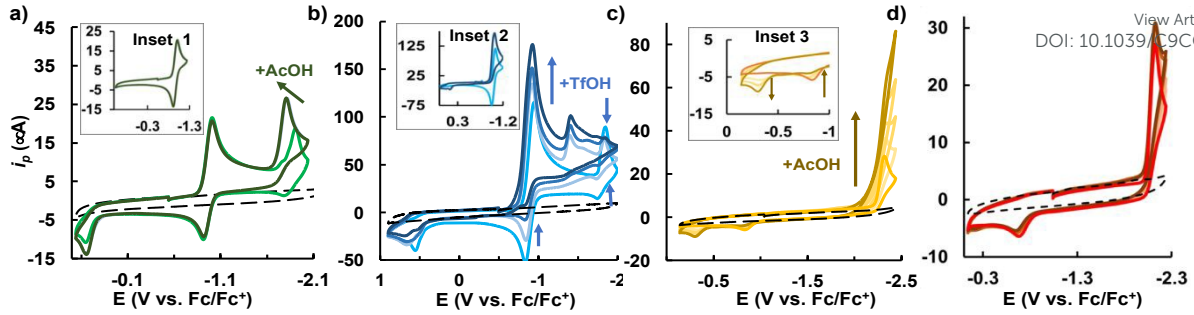

Figure 1 Cyclic voltammograms of: a) 2 mM A_2^+ in the presence of 0-60 eq AcOH in DMSO; b) 5 mM A_2^+ in the presence of 0-1 eq TfOH in MeCN; c) 2 mM B_3^+ in the presence of 0-60 eq AcOH in DMSO; d) 2 mM B_2^+ in the presence of 0-60 eq AcOH in DMSO. Arrows indicate the direction of peak changes with the addition of acid, while black dashed curves represent baseline scans.

nes with two well-separated reduction peaks (Fig S2). In contrast, upon addition of acetic acid the current density at the first reduction potential increases and the current density at the second reduction potential decreases, indicating a shift from the EEP to the EPE route. The EPE process presumably occurs via a stepwise mechanism consistent with the absence of a kinetic isotope effect when deuterated acetic acid is used (Fig S13b). The stepwise mechanism likely results from the low tendency of carbon-based radicals to form hydrogen bonds. This behavior is unlike that observed in nitrogen- and oxygen-based radicals, where hydrogen bonding occurs to pre-associate proton donors and acceptors and to facilitate the concerted reduction of flavins and quinones/phenols.[5b-5e, 13]

Lastly, we address why benzimidazole radicals are drastically more reactive towards protons than acridines, although they are seemingly structurally similar (i.e. both are N-heterocyclic species). Electron-donating substituents decrease the acidity of radical cations,[8c] as Table 1 indicates. However, the sensitivity of acidity to functionalization for both classes is limited to a few pK_a units. Various acridine-based radicals were only protonated by very strong acids, indicating that the radical cation remains extremely acidic regardless of functionalization. The large difference in the acidities of radical cations can be attributed to the stability of the radicals (Fig 2), where cyclopentyl radicals (benzimidazoles) are more destabilized by ring strain relative to cyclohexyl radicals (acridines).[14] This is further supported by our calculated 'strain energies' of two representative derivatives.[15] Protonation of the singly-reduced radical intermediates R· of both classes requires reorganization of the molecular structure, as indicated by the angular differences between R· and RH^+· (see Fig 2). Acridine-based compounds undergo a more pronounced structural relaxation upon protonation, whereas the reorganization associated with protonating benzimidazole radicals is minimal; The energy penalty of straining the geometry of the radical species is ~17 kcal/mol for the acridine derivative A_5· but only ~8 kcal/mol for the benzimidazole intermediate B_3·, indicating that protonation of acridine derivatives requires a larger driving force.

The computed energy profiles for the regeneration of two representative hydrides with similar hydricities (A_5H and B_3H, ΔG_{H-} = ~45-47 kcal/mol, Table 1) reveals several key principles for their electrochemical conversions (Fig 2). First, as evident from Fig 2 and supported by our experimental findings, acridines prefer the EEP route unless coupled with very strong acids ($pK_a << 0$, DMSO). In contrast, benzimidazoles proceed facilely via the EPE path even with relatively weak acids. Second, the regeneration of both classes of hydrides necessitates an overpotential for their successful transformation. The "ideal" system would operate at the thermodynamic potential (− 1.3 V vs. Fc/Fc^+),[16,17] while the required applied potential (E_{app}) for generation of both representatives is slightly more negative. Specifically, the generation of A_5H is determined by $E^0_{R\cdot/R^-}$ due to the difficult radical protonation (E_{app} = − 2.4 V vs Fc/Fc^+), whereas B_3H is generated at $E^0_{R+/R\cdot}$ with an appropriate proton donor (E_{app} = − 2.3 V vs Fc/Fc^+). We emphasize that the overpotential is not affected by the basicity of the radical species. Instead, it only depends on the first reduction potential ($\boldsymbol{E_{app} = E^0_{R^+/R\cdot}}$) for benzimidazoles because they follow the EPE route, and the second reduction potential ($\boldsymbol{E_{app} = E^0_{R\cdot/R^-}}$) for acridines, as they favour the EEP route. This outcome indicates that the structural factors that facilitate the radical protonation of benzimidazoles – as defined by $pK_a(RH^+\cdot)$ – also impede the first reduction process, as defined by $E^0_{R+/R\cdot}$, leading to an overall compensating effect on the thermodynamics of hydride generation (Fig S14).

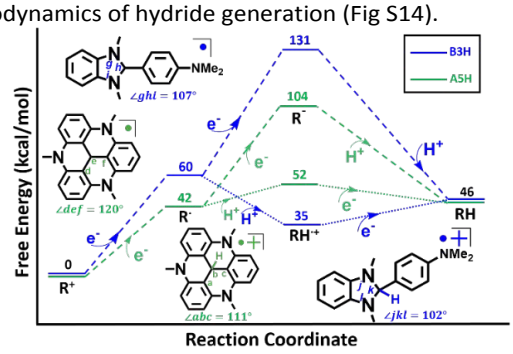

Figure 2 EEP and EPE reaction coordinate diagram for B_3H (blue, benzimidazole) and A_5H (green, acridine). $B_3\cdot^{/H+}$ and $A_5\cdot^{/H+}$ structures with angles below to show geometric changes. (See ESI for calculation details).

While the mechanisms have no effect on the overall reaction free energy to generate the hydrides, we suggest that the EEP and EPE routes likely exhibit different kinetics. This is also true for the kinetics of undesirable side reactions, especially for those that involve the intermediates produced by the two mechanisms. Exploiting the differences in the kinetics of the two mechanisms can be highly advantageous. For example, the dimerization of open-shell radicals R· formed by the first electron transfer significantly lowers the efficiency of hydride regeneration via EEP mechanisms. However, rapid protonation of R· lowers its concentration and consequently the rate of the bimolecular dimerization reaction with $\boldsymbol{r_{dim} \propto [R\cdot]^2}$. Indeed, our experiments clearly demonstrate that the

EPE mechanism where protonation of the radical successfully outcompetes dimerization enables quantitative hydride recovery. Thus, the EPE mechanism is likely more suitable for catalytic systems that involve reductions by organic hydrides.

To conclude, the experiments and calculations in this work support our hypothesis that the acidity of the radical cation ($RH^{+\cdot}$) of organic hydrides is critical for determining the pathway of electrochemical hydride generation. A detailed analysis of the factors that determine radical stability (and correspondingly its basicity) demonstrates how structural modification can tune the hydride regeneration mechanism. In contrast, the different hydride generation pathways (EEP vs. EPE) do not affect the overall potential required for the complete regeneration, due to the opposing effects that radical stability plays on electrochemical potentials and pK_a values. Thus, despite its identical thermodynamic requirements, the EPE mechanism observed in benzimidazoles is likely more efficient due to the suppression of undesired radical dimerization. This work provides the groundwork for a more effective use of organic hydrides as catalysts.

This work was supported by the ACS Petroleum Research Fund (PRF; Grant 54436-ND4) and Kuwait University Fellowship. The computational work was achieved with the help of the Advanced Cyberinfrastructure for Education and Research (ACER) center at the University of Illinois at Chicago.

Conflicts of interest

There are no conflicts to declare.

Notes and references

1. (a) T. J. Meyer, M. H. V. Huynh and H. H. Thorp, *Angew. Chem*, 2007, **46**, 5284-5304; (b) M. H. V. Huynh and T. J. J. C. R. Meyer, *Chem. Rev.*, 2007, **107**, 5004-5064; (c) D. R. Weinberg, C. J. Gagliardi, J. F. Hull, C. F. Murphy, C. A. Kent, B. C. Westlake, A. Paul, D. H. Ess, D. G. McCafferty and T. J. Meyer, *Chem. Rev.*, 2012, **112**, 4016-4093.

2. (a) P. M. Zimmerman, Z. Zhang and C. B. Musgrave, *Inorg. chem.*, 2010, **49**, 8724-8728; (b) C.-H. Lim, A. M. Holder, J. T. Hynes and C. B. Musgrave, *J. Am. Chem. Soc.*, 2014, **136**, 16081-16095; (c) C.-H. Lim, A. M. Holder, J. T. Hynes and C. B. Musgrave, *J. Phys. Chem. Lett*, 2015, **6**, 5078-5092.

3. (a) M. L. Helm, M. P. Stewart, R. M. Bullock, M. R. DuBois and D. L. DuBois, *Science*, 2011, **333**, 863-866; (b) X. Hu, B. S. Brunschwig and J. C. Peters, *J. Am. Chem. Soc.*, 2007, **129**, 8988-8998; (c) E. S. Rountree and J. L. Dempsey, *J. Am. Chem. Soc.*, 2015, **137**, 13371-13380; (d) A. Taheri, E. J. Thompson, J. C. Fettinger and L. A. Berben, *ACS Catal.*, 2015, **5**, 7140-7151; (e) S. Roy, B. Sharma, J. Pécaut, P. Simon, M. Fontecave, P. D. Tran, E. Derat and V. Artero, *J. Am. Chem. Soc.*, 2017, **139**, 3685-3696; (f) S. E. Witt, T. A. White, Z. Li, K. R. Dunbar and C. Turro, *Chem. Comm.*, 2016, **52**, 12175-12178; (g) N. D. Loewen, E. J. Thompson, M. Kagan, C. L. Banales, T. W. Myers, J. C. Fettinger and L. A. Berben, *Chem. Sci.*, 2016, **7**, 2728-2735; (h) A. D. Nguyen, M. D. Rail, M. Shanmugam, J. C. Fettinger and L. A. Berben, *Inorg. Chem*, 2013, **52**, 12847-12854.

4. (a) E. S. Rountree, D. J. Martin, B. D. McCarthy and J. L. Dempsey, *ACS Catal.*, 2016, **6**, 3326-3335; (b) E. S. Wiedner, H. J. Brown and M. L. Helm, *J. Am. Chem. Soc.*, 2016, **138**, 604-616; (c) D. K. Bediako, B. H. Solis, D. K. Dogutan, M. M. Roubelakis, A. G. Maher, C. H. Lee, M. B. Chambers, S. Hammes-Schiffer and D. G. Nocera, *Proc. Natl. Acad. Sci. U.S.A*, 2014, **111**, 15001-15006; (d) J. T. Muckerman and E. Fujita, *Chem. Comm.*, 2011, **47**, 12456-12458; (e) N. m. Elgrishi, D. A. Kurtz and J. L. Dempsey, *J. Am. Chem. Soc.*, 2016, **139**, 239-244.

5. (a) C. Costentin, *Chem. Rev.*, 2008, **108**, 2145-2179; (b) N. Gupta and H. Linschitz, *J. Am. Chem. Soc.*, 1997, **119**, 6384-6391; (c) E. Breinlinger, A. Niemz and V. M. Rotello, *J. Am. Chem. Soc.*, 1995, **117**, 5379-5380; (d) L. Hammarström and S. Styring, *Energy Environ. Sci.*, 2011, **4**, 2379-2388; (e) L. O. Johannissen, T. Irebo, M. Sjödin, O. Johansson and L. Hammarström, *J. phys. Chem. B*, 2009, **113**, 16214-16225.

6. (a) B. H. Solis, A. G. Maher, D. K. Dogutan, D. G. Nocera and S. Hammes-Schiffer, *Proc. Natl. Acad. Sci. U.S.A*, 2016, **113**, 485-492; (b) H. Ohtsu and K. Tanaka, *Angew. Chem*, 2012, **51**, 9792-9795; (c) Y. Matsubara, S. E. Hightower, J. Chen, D. C. Grills, D. E. Polyansky, J. T. Muckerman, K. Tanaka and E. Fujita, *Chem. Comm.*, 2014, **50**, 728-730; (d) D. E. Polyansky, D. Cabelli, J. T. Muckerman, T. Fukushima, K. Tanaka and E. Fujita, *Inorg. Chem*, 2008, **47**, 3958-3968; (e) P. A. Karplus, M. J. Daniels and J. R. Herriott, *Science*, 1991, **251**, 60-66; (f) B. H. Solis, A. G. Maher, T. Honda, D. C. Powers, D. G. Nocera and S. Hammes-Schiffer, *ACS Catal.*, 2014, **4**, 4516-4526.

7. (a) A. Anne, S. Fraoua, V. Grass, J. Moiroux and J.-M. Savéant, *J. Am. Chem. Soc.*, 1998, **120**, 2951-2958; (b) J. Zielonka, A. Marcinek, J. Adamus and J. Gebicki, *J. Phys. Chem. A*, 2003, **107**, 9860-9864; (c) J. Hermolin, M. Levin and E. M. Kosower, *J. Am. Chem. Soc.*, 1981, **103**, 4808-4813; (d) G. de Robillard, C. H. Devillers, D. Kunz, H. Cattey, E. Digard and J. Andrieu, *Org. Lett.*, 2013, **15**, 4410-4413; (e) A. Anne, P. Hapiot, J. Moiroux and J.-M. Savéant, *J. Electroanal. Chem.*, 1992, **331**, 959-970; (f) P. Hapiot, J. Moiroux and J. M. Saveant, *J. Am. Chem. Soc.*, 1990, **112**, 1337-1343.

8. (a) S. Ilic, U. Pandey Kadel, Y. Basdogan, J. A. Keith and K. D. Glusac, *J. Am. Chem. Soc.*, 2018, **140**, 4569-4579; (b) S. Ilic, A. Alherz, C. B. Musgrave and K. D. Glusac, *Chem. Soc. Rev.*, 2018, **47**, 2809-2836; (c) A. Alherz, C.-H. Lim, Y.-C. Kuo, P. Lehman, J. Cha, J. T. Hynes and C. B. Musgrave, *J. Phys. Chem. B*, 2018, **122**, 10179-10189; (d) A. Alherz, C.-H. Lim, J. T. Hynes and C. B. Musgrave, *J. Phys. Chem. B*, 2018, **122**, 1278-1288.

9. C.-H. Lim, S. Ilic, A. Alherz, B. T. Worrell, S. S. Bacon, J. T. Hynes, K. D. Glusac and C. B. Musgrave, *J. Am. Chem. Soc.*, 2018, **141**, 272-280.

10. (a) S. Ilic, E. S. Brown, Y. Xie, S. Maldonado and K. D. Glusac, *J. Phys. Chem. C*, 2016, **120**, 3145-3155; (b) G. N. Hargenrader, R. B. Weerasooriya, S. Ilic, J. Niklas, O. G. Poluektov and K. D. Glusac, *ACS Appl. Energy Mater.*, 2018, DOI: 10.1021/acsaem.8b01574.

11. E. S. Wiedner, M. B. Chambers, C. L. Pitman, R. M. Bullock, A. J. Miller and A. M. Appel, *Chem. Rev.*, 2016, **116**, 8655-8692.

12. The appearance of the irreversible peak at -1.5 V is discussed in ESI Section E2.

13. (a) T. F. Markle, I. J. Rhile and J. M. Mayer, *J. Am. Chem. Soc.*, 2011, **133**, 17341-17352; (b) I. J. Rhile and J. M. Mayer, *J. Am. Chem. Soc.*, 2004, **126**, 12718-12719.

14. H. Zipse, *To. in Curr. Chem*, 2006, **263**, 163.

15. The strain energy is defined as the free energy difference between the relaxed geometry of the radical (R·) and the deprotonated cationic radical intermediates. Larger strain energies correspond to larger acidities (lower pKa values) since the radical (conjugate base) must undergo a more drastic structural change.

16. The ideal reduction potential for the hydride regeneration ($R^+ + 2e^- + H^+ \rightarrow RH$) was calculated using the hydricity ΔG_{H-} 45 kcal/mol ($RH \rightarrow R^+ + H^-$) and DG for the reaction: $H^+ + 2e^- \rightarrow H^-$ (from ref 16).

17. K. L. Handoo, J. P. Cheng and V. D. Parker, *J. Am. Chem. Soc.*, 1993, **115**, 5067-5072.